AGU PUBLICATIONS

Geophysical Research Letters

RESEARCH LETTER
10.1002/2015GL066030

Key Points:
- One-second sampling at NOAA tide gauges measures local wind/swell and infragravity waves
- Harbor and ocean-pier sample standard deviations are correlated to offshore wave heights
- A combined water level sample mean and standard deviation provide a dynamical water level estimate

Supporting Information:
- Tables S1 and S2 and Figure S1

Citation:
Sweet, W. V., J. Park, S. Gill, and J. Marra (2015), New ways to measure waves and their effects at NOAA tide gauges: A Hawaiian-network perspective, *Geophys. Res. Lett.*, *42*, 9355–9361, doi:10.1002/2015GL066030.

Received 1 SEP 2015
Accepted 20 OCT 2015
Accepted article online 26 OCT 2015
Published online 11 NOV 2015

New ways to measure waves and their effects at NOAA tide gauges: A Hawaiian-network perspective

William V. Sweet[1], Joseph Park[2], Stephen Gill[1], and John Marra[3]

[1]NOAA Center for Operational Oceanographic Products and Services, Silver Spring, Maryland, USA, [2]National Park Service, Homestead, Florida, USA, [3]NOAA National Center for Environmental Information, Honolulu, Hawaii, USA

Abstract We use the standard deviation (sigma) of continuous 1 s water level sampling at 46 U.S. NOAA tide gauges available since 1996 as a high-frequency variance measure. Sigma estimates local infragravity and incident wave band variability, is significantly correlated ($r = 0.5$–0.9) to significant wave height (H_s), and scales linearly to local observations and output from the global ocean wave reanalysis at most ocean-exposed and harbor-sheltered locations. Empirical orthogonal functions of daily mean sigma from six Hawaii tide gauges distinguish northerly and southerly modes that closely match local Hs observations. Depending on tide gauge location, the 99% of daily maxima sigma can be as large as or larger than the nontidal residual component of the water level sample. Our findings provide new uses of land-based tide gauge data to estimate significant wave heights and dynamic water levels to better monitor for local conditions leading to impacts.

1. Introduction

Coastal communities are increasingly at risk from high-water events [*Salas and Obeysekera*, 2013; *Sweet and Park*, 2014], whose flooding and erosion threaten homes, public works and infrastructure, freshwater resources, harbor operations, etc. Since tide gauges (TG) are located at the land-sea interface, they are an optimal platform to monitor for damaging water levels. TGs offer decadal and longer-scale observations of water levels that support hazard-to-climate investigations of storm surge [*Zhang et al.*, 2000; *Bromirski et al.*, 2003], ocean circulation [*Ezer*, 2015] and sea level rise [*Merrifield et al.*, 2012; *Church et al.*, 2013].

TGs are designed to record slow changes in water level. Due to the mechanical low-pass filtering associated with their protective wells, multi minute averaging scheme and general placement in protected waters, their data are considered a still water level (SWL) estimate:

$$\mathrm{SWL}(t) = \mathrm{MSL}_{\mathrm{Datum}} + \mathrm{tide}(\mathrm{astronomic},\ \mathrm{MSL\ cycle}) + \mathrm{NTR}\ (\mathrm{storm\ surge},\ \mathrm{anomaly},\ \mathrm{wave\ setup}) \quad (1)$$

defined as a water level height averaged over sampling period, t, relative to mean sea level (MSL) or an appropriate tidal datum [*CO-OPS*, 2001], a tidal contribution usually consisting of the astronomical tide and a MSL seasonal/annual constituent and a nontidal residual (NTR) representing localized storm surge, any prior-existing sea level anomaly and wave setup if present during sampling from breaking waves in the surf zone and within coral-reef lagoons [*Vetter et al.*, 2010] and atolls [*Aucan et al.*, 2012].

Hydraulic impacts, on the other hand, during extreme water level events [*Tebaldi et al.*, 2012; *Zervas*, 2013] result from more of an instantaneous total water level (TWL; H. Mortiz, et al. (2015), U.S. Army Corp of Engineers Adaptation Approach for Future Coastal Climate Conditions, J. of ICE Maritime Engineering, in press.), which include higher-frequency (seconds - min) wave processes typically associated with runup effects on a sloping beach. TG platforms are located at the land-ocean interface (i.e., docks, seawalls, piers) and typically do not experience such swash-related motions. A TG without consideration of its averaging scheme and physical dampening from its protective structure experiences more of a dynamic water level (DWL):

$$\mathrm{DWL}(t) = \mathrm{SWL} + \alpha^{*}\mathrm{sigma} \quad (2)$$

where SWL is obtained from equation (1), α is an exceedance duration coefficient associated with the sampling period (e.g., 1.96 approximates the 95% of the Gaussian distribution) and sigma represents the standard deviation of the high-frequency oscillations that directly impinge upon TG platforms from incident ($\mathrm{wave}_{\mathrm{inc}}$) wind waves/swell (periods of 5–25 s) generally attenuated in harbors by design and by longer-period (25 s to tens of minutes) infragravity waves ($\mathrm{wave}_{\mathrm{ig}}$) often pronounced in harbors

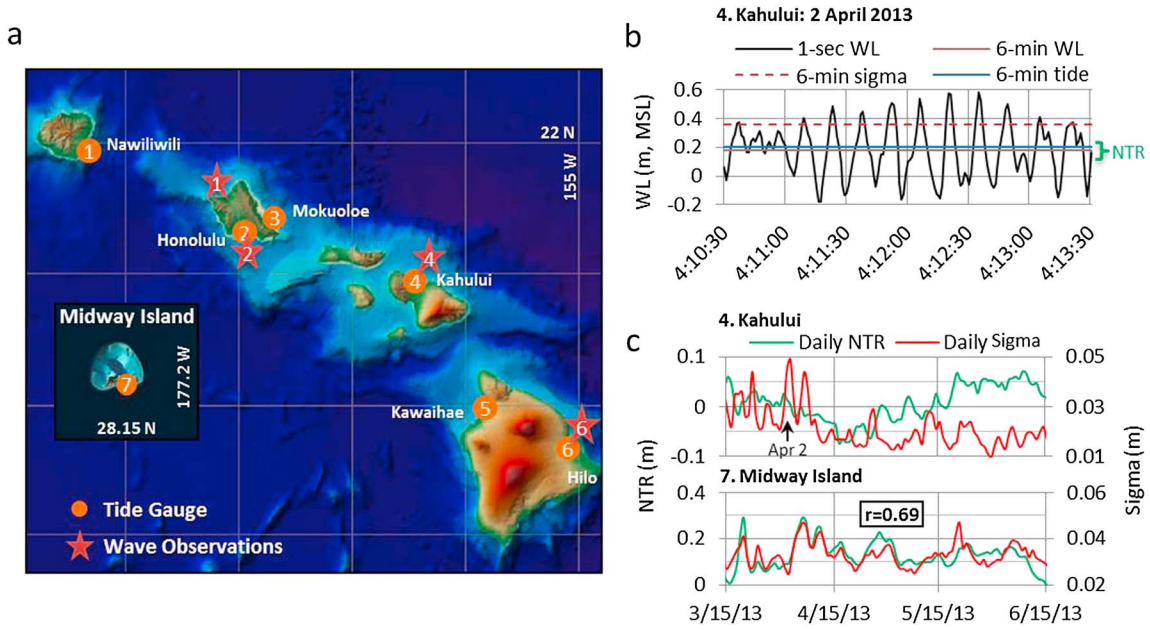

Figure 1. (a) Map of NOAA tide gauge (TG; orange circles) and wave (red stars) locations in the Hawaiian Islands and Midway Island; (b) 1 s water level sampling (black) by a Seabird instrument co-located at TG 4 (Kahului) on 2 April 2013 showing the 181 1 s sample mean (0.18 m, red line) relative to NOAA's MSL datum, NOAA tide prediction (0.2 m, blue), NTR (−0.02 m and signified by green bracket), and sigma (0.18 m above mean, red dash); (c) 3 months of daily-averaged NTR and sigma at TG 4 and at Midway Island with their linear-regression correlation coefficient (r) shown where significant at 99% level (p value < 0.01).

[*Thotagamuwage and Pattiaratchi*, 2014; *Park et al.*, 2015]. The magnitude of sigma is presumably dependent upon the TG location. Estimates of DWLs and TWLs typically require additional data (e.g., wave buoy or model output) and more complex methods to determine. Wave-related impacts are the primary concern within the Pacific [*Marra et al.*, 2012], such as island overwash that occurs when large swells hit during seasonally high tides [*Hoeke et al.*, 2013]. Along the U.S. West Coast, such events cause extensive erosion [*Barnard et al.*, 2011] and increasing significant wave heights (H_s) over the last couple decades have been more of a factor than sea level rise [*Ruggiero*, 2013].

Here we utilize the standard deviation ("sigma") computed during water level sampling as a physical measurement instead of its intended use as a SWL performance metric at U.S. National Oceanic and Atmospheric Administration (NOAA) TGs. Sigma estimates water level variability occurring over the $\text{wave}_{\text{inc}} + \text{wave}_{\text{ig}}$ bands, and together with the reported TG "mean" value, quantifies instantaneous exposure levels and durations above a reference elevation. We show that daily mean TG sigma is (1) highly sensitive to and can provide a local approximation for H_s and (2) is a major DWL component at exposed (e.g., ocean piers) and harbor TG locations. Our findings offer novel approaches for monitoring local wave and water level conditions and extend earlier TG satellite [*Parke and Gill*, 1995] and next-generation sensor performance [*Park et al.*, 2014a] comparison studies.

2. Study Area and Data

We use hourly TG measurements from NOAA (www.tidesandcurrents.noaa.gov) and specifically those collected since ~1996, which include the water level (mean) and its sample standard deviation (sigma). Both estimates are derived from 181 continuous 1 s samples collected every 6 min (i.e., "3 min on and 3 min off" sampling scheme) from an acoustic-based sensor inside a protective well, which is designed to mechanically dampen water level oscillations with periods ≤5 s [*Park et al.*, 2014a]. We recognize that this sampling strategy leaves oscillations with 3–6 min unresolved. NTR values are obtained by subtracting the local NOAA tide predictions from the water level observations at each TG. We analyze wave-related responses (1) regionally across the Hawaiian Islands Region, (2) locally at three Hawaiian TGs (sites 2, 4, and 6; Figure 1a) where Seabird 26Plus wave and water level recorders with Paroscientific Digi-quartz pressure instruments sampling at a 1 s rate were codeployed near NOAA TGs by the University of Hawaii Sea Level Center and

(3) nationally at 43 NOAA TGs whose long-term average sigma is >2 cm as well as at three additional TG locations in the HI Islands. It should be noted that archived NOAA TG records are verified by a quality assurance procedure using a 3-sigma threshold designed to reject anomalous 1 s water level samples after which the final water level average is computed; sigma values themselves, however, are not verified or rejected. As such, there can be erroneous (order of magnitude) spikes and "zeros" in the records, which we remove by filtering all sigma >99.8% of the daily maximum values and all sigma values equal to 0. Additional TG and wave-data information is provided in Tables S1 and S2 in the supporting information.

TG water level sigma are compared to nondirectional H_s recorded by buoys (wave sites 1, 4, and 6; https://cdip.ucsd.edu) and at wave site 2, whose hourly H_s is approximated as 4*standard deviations of hourly 1 s samples obtained by a SBE26 Plus. We also utilize hourly nondirectional H_s from the global ocean wave (GOW) reanalysis over 1996–2013 [*Perez et al.*, 2015], which is based upon the WaveWatch III wave model [*Tolman*, 2014]. The model has a $1° \times 1.5°$ spatial resolution, and H_s are considered an offshore estimate. Nearest model output directly offshore each NOAA TG is used. Although the Hawaiian Island topography is not resolved by the model, obstruction grids are included in the numerical simulation using the approach described in *Chawla and Tolman* [2008].

3. Findings

3.1. TG Water Level Mean and Sigma Parameters

The HI Islands are located in the central North Pacific (Figure 1a) and subjected to several directional surface gravity wave climatologies [*Bromirski et al.*, 2005; *Aucan*, 2006] that cause substantial variability during NOAA TG sampling. Figure 1b shows a record of 181 1 s water level samples made by our Seabird instrument co-located at the NOAA TG 4 (Kahului) on 2 April 2013 at 04:12:00 with the resultant 3 min sample mean, NTR (difference between water level and tide), and sigma values. This sample occurred during a large northerly swell (shown in Figure 3b), and the 1 s water level data reveal distinct 15 s oscillations with amplitudes of 0.6 m. Figure 1c shows daily mean NTR and sigma values recorded by NOAA TGs in Kahului and Midway Atoll. At Kahului, high sigma values do not translate into higher NTR (no correlation) even when very large water level oscillations are present in the harbor. On the other hand, NTR and sigma are well correlated ($r = 0.69$; p value < 0.01) at Midway Island, a phenomenon quite rare for NOAA TGs, which is attributed to wave setup from breaking waves that drive water over the reef, raising levels within the atoll lagoon [*Aucan et al.*, 2012] as well as increased variability during sampling.

3.2. Spatial Signature of Sigma and Regional Wave Climatology

When analyzed regionally via empirical orthogonal functions (EOFs), sigma measured by a network of TGs distinguishes distinct wave climatologies impacting Hawaii. The first EOF explains 42% of the signal variance and is a mode representing the northerly wavefield impacting TGs that are north facing (TGs 4 and 6) or north sensitive (TG 5) (Figure 2a). The principle component (PC) for EOF mode 1 has a very similar pattern to the seasonal storm and predominant wave climatology in the north Pacific [*Aucan*, 2006], which is highest in the boreal winter and smallest during summer (Figure 2b). Daily mean time series of PC 1 and H_s recorded at wave site 2 off of the north shore of Oahu (which is shielded to all but northerly waves) are significantly correlated ($r = 0.79$; p value < 0.01) as shown in Figure 2c. The second EOF explains 22% of the signal variance and is a mode primarily experienced at southern facing TGs 1 and 2. Opposite to PC 1, PC 2 has a seasonal distribution that peaks in boreal summer (i.e., austral winter) and is lowest in winter (Figure 2b). Its high correlation ($r = 0.83$) to H_s measured for several months off Oahu's south shore at wave site 2 (Figure 2d) indicates that EOF 2 is capturing swell generated in the Southern Hemisphere, which is largest during the austral winter-storm season.

3.3. Local H_s and TG Water Level Response

Our high-resolution sampling focuses on the harbors of Honolulu (TG 1), Kahului (TG 4), and Hilo (TG 6), where we make comparisons to H_s measured by in situ platforms (Table S2). Multimonth records of 1 s water levels recorded by the Seabird instrumentation co-located at the NOAA TGs capture the harbor response to increasing H_s (Figure 3). As daily H_s increases in each harbor, there is no discernable concurrent daily water level setup (no NTR correlation; Figure 3, top). However, daily sigma is correlated ($r \sim 0.78$, p value < 0.01) to the changing

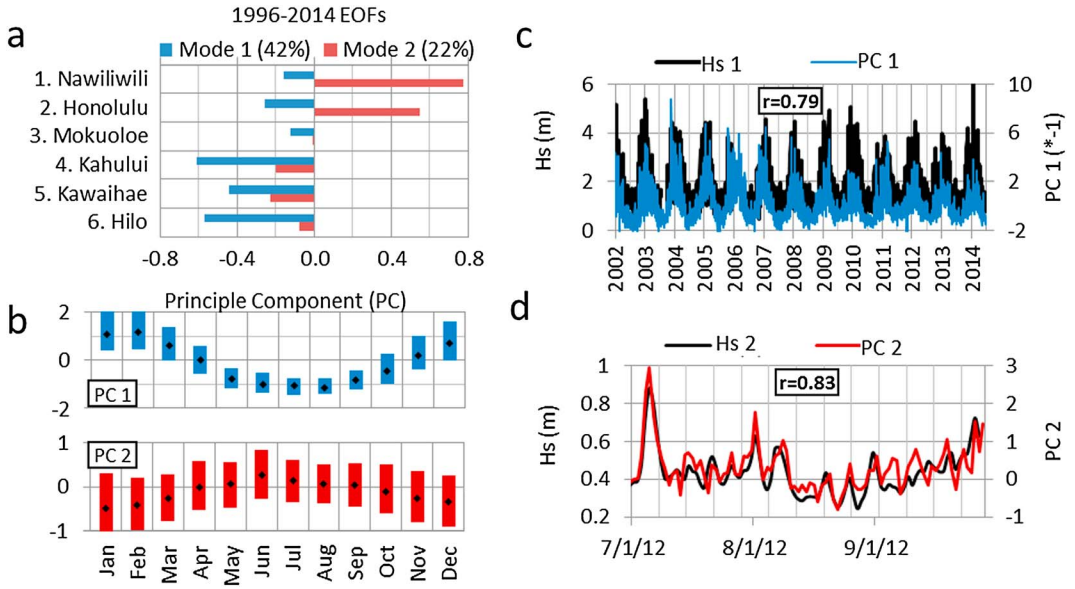

Figure 2. (a) Empirical orthogonal functions (EOFs) for the first two modes of daily mean WL sigma from 1996 to 2014 from NOAA Hawaiian TGs, each normalized to unit variance. The percent of the variance explained by each mode is shown in parentheses. (b) Seasonal-distribution box plots (median-dot and first and third quartile-colored box) of the principle component (PC) time series for EOF modes 1 and 2. PC time series are shown in (c) for EOF mode 1 (blue) with H_s from wave buoy (1) off of north shore of Oahu, and in (d) for EOF mode 2 (red) with H_s from wave buoy (2) off of south shore of Oahu. Correlation coefficients from linear regression are shown and are significant at the 99% level (p value < 0.01).

offshore H_s. We use daily mean values to illustrate the relationship, but note that similar patterns exist but with progressively weakened correlation strength when using shorter averaging spans (e.g., 1–24 hours).

Each harbor oscillates at several $wave_{inc} + wave_{ig}$ bands as shown in the respective spectrogram (Figure 3, bottom), which are composed of daily spectral densities estimated by the *Welch* [1967] method with a 12 h sliding window. The spectra show that the harbors experience relatively continuous swell energy at event-specific periods (<25 s). The spectra also reveal several horizontal bands at periods much longer than wind waves associated with wave-forced standing waves ($wave_{ig}$) likely specific to pier structures and harbor dimensions (periods < 600 s). $Wave_{ig}$ associated with shelf dimensions (periods > 600 s) are more persistent and presumably a resonance driven by tidal energy [*Woodworth et al.*, 2005; *Wijeratne et al.*, 2010]. The wave-forced $wave_{ig}$ (harbor oscillations) are similar to those discussed by *Thotagamuwage and Pattiaratchi* [2014] in Two Rocks, Australia, and *Park et al.* [2015] in Monterey, CA. Although Honolulu (Figure 3a) was sampled under smaller H_s conditions (daily averages less than 1 m), its harbor appears a better spatial filter of $wave_{inc}$ energy as compared to Kahului (Figures 1b and 3b) and Hilo (Figure 3c), where large spectral peaks exist in $wave_{inc}$ bands during high H_s events. All three harbors possess similar linear regression coefficients of ~0.01 between daily mean H_s and sigma (both expressed in meters), implying that for every 1 m increase in H_s, sigma increases by ~1 cm on average.

3.4. National Relationships

3.4.1. GOW H_s and TG Water Level Sigma

Water level sigma measured at NOAA TGs around the U.S. reveal a high degree of sensitivity to wave forcing at both ocean-exposed (pier) and harbor-sheltered locations (Figure 4a and Table S1). Linear regression between daily mean GOW H_s and TG sigma over 1996–2014 or maximum period of TG record (Table S1) are correlated ($r = 0.5$–0.9 above the 99% significance level; p values < 0.01) at the majority of the study's TGs. The amount of landward attenuation between offshore H_s to shore-measured TG sigma is related to its linear regression coefficient, with differences presumably from regional topo-bathymetric characteristics and TG placement/exposure. For example, along the U.S. West Coast where H_s and sigma have highest correlations ($r = 0.7$–0.9), the regression coefficients have broad similarities (blue and green dots, Figure 4a) with sigma increasing by 1–5 cm locally for every 1 m rise in H_s. Higher coefficient values (>0.05) along the U.S. East Coast

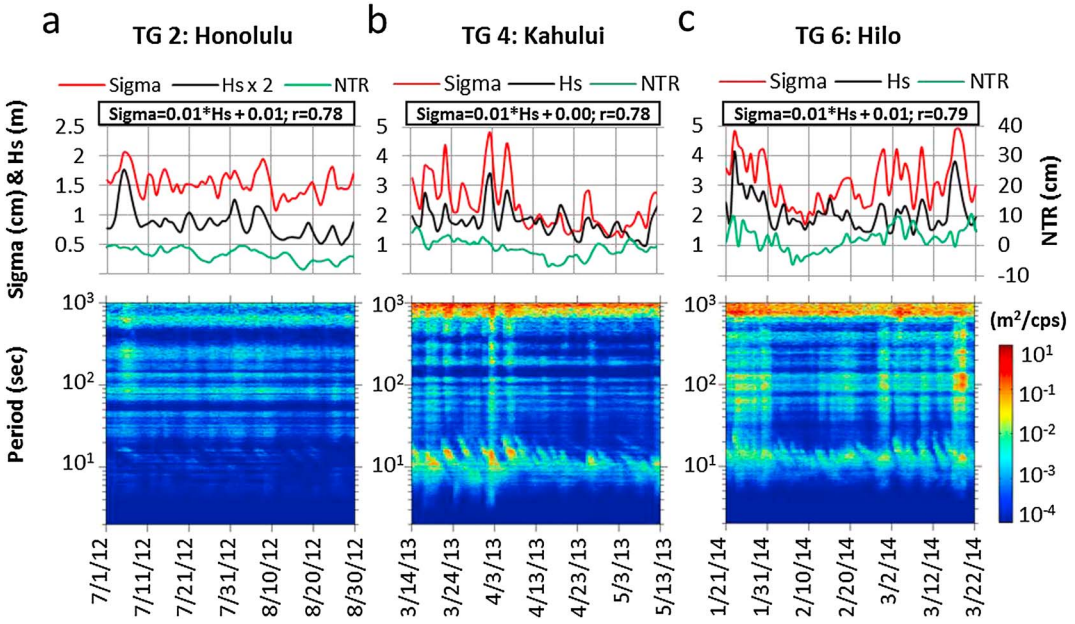

Figure 3. Daily mean in situ measured H_s and NOAA TG NTR and sigma concurrent with spectrogram of 1 s water level data at TGs in (a) Honolulu, (b) Kahului, and (c) Hilo with power spectral density by Welch Method. Linear regression results are shown with the correlation coefficient (r) significant at 99% level (p value < 0.01) based upon 60 day series and sigma in meters.

are found at exposed ocean-pier mounted TGs. The two locations with highest regression coefficients (red dots, 0.075–0.1) are on piers in Wrightsville Beach, NC, and La Jolla, CA. The GOW-derived coefficients based upon daily mean H_s for the Hawaiian TGs are 2–3 times larger at TGs 4 (Kahului) and 6 (Hilo) and about a third of the magnitude at TG 2 (Honolulu) than as estimated using daily mean H_s measured locally (Figure 3) likely related to the longer period for comparison and difficulties in resolving the complex HI topography.

3.4.2. Relative Magnitude of Water Level NTR and Sigma

Wave-related variability can be quite large during NOAA TG sampling (e.g., Figure 1b) with daily maximum sigma values >0.3 m not uncommon throughout the year (Table S1). We provide a ratio comparing the 99% of daily maxima over the period of record derived from hourly NTR and sigma values in Figure 4b. This ratio assesses the magnitude of $wave_{inc}$ and $wave_{ig}$ during large annual events as compared to the NTR (~storm surge) component. A similar ratio comparing TG astronomical tidal and NTR components (i.e., in equation (1)) quantifies the overall importance of storm surge and tide range during annual extremes [*Merrifield et al.*, 2013; *Sweet et al.*, 2014]. Along the East Coast, where large storm surges occur, NTR is 1 to 5

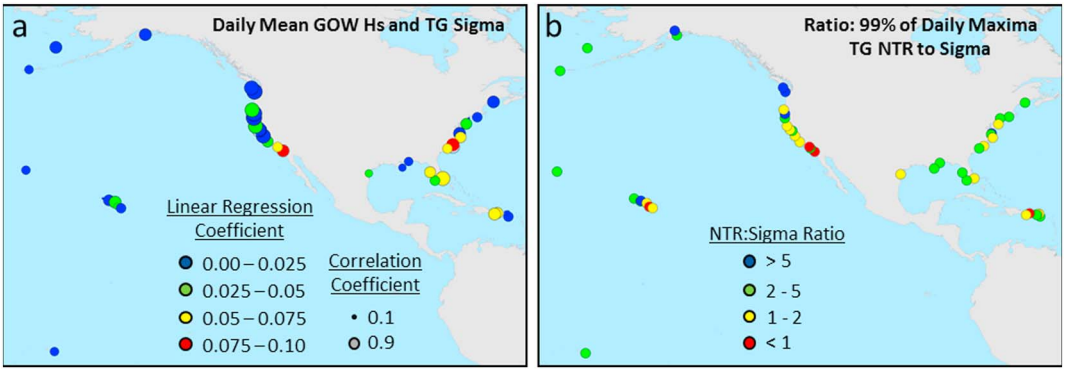

Figure 4. (a) The 1996–2013 linear regression between daily mean global ocean wave (GOW) model H_s and daily mean tide gauge (TG) sigma showing coefficient (color) and correlation (size) significant at 99% level (p value < 0.01) and (b) the ratio between the 99% of daily maxima of hourly NTR and sigma values.

times larger than sigma's magnitude during such events. Along the West Coast and in some HI and Caribbean harbors where continental shelves are narrower, however, sigma is on par and/or greater (ratio < 1) than the NTR component itself.

4. Summary Remarks

Due to their maritime history, TGs have been purposely engineered to measure slow-changes in water levels. Here we use the standard deviation (sigma) computed during sampling at NOAA TGs as a dynamical measurement of wave-related variability present during sampling. TG sigma is correlated ($r = 0.5$–0.9) with changing offshore (nondirectional) H_s at ocean-pier and harbor TG locations around the U.S. One-second water level samples at three HI Island TGs show that $wave_{inc}$ and $wave_{ig}$ modulate in response to changing H_s and their correlations are higher ($r > 0.7$–0.8) when comparing to in situ measured H_s than using modeled H_s likely from the course GOW model resolution. Relationships are further enhanced ($r > 0.9$) when comparing water level sigma obtained from the bottom-mounted Seacat sensors without a protective well (Honolulu) or when applying a 10–22 s band-pass filter to the wind/swell H_s (Kahului and Hilo). Directional H_s information is obtained through EOF spatial analysis of sigma from a network of Hawaiian TGs that distinguish a northerly and southerly H_s mode that closely match ($r \sim 0.8$) local H_s time series and their season climatologies. With sufficient local calibration, TG sigma shows promise as an estimator for local offshore H_s.

Coefficients between daily average H_s and TG sigma reveal regional attenuation patterns (Figure 4a), such as along the U.S. West Coast (Figure 4a), where wave-related effects and DWLs are of greater concern during extreme events (Figure 4b). Additional factoring by an exceedance coefficient (α) in equation (1) provides duration estimates of DWLs over a measurement period. For instance, a DWL expected to occur 95% of a given time period could be estimated by the TG sample mean (SWL) + 1.96*sigma, assuming a Gaussian distribution of 1 s sampling, which is generally found to be the case (not shown). Such observational-based DWL estimates should improve impact climatologies and help validate nearshore water level-wave models.

We recognize that sigma is only a partial estimate of $wave_{inc}$ and $wave_{ig}$ variability at a TG location due to its sampling scheme, which does not fully resolve oscillations with periods between 3 and 6 min. Sigma as reported (181 1 s samples every 6 min) is >95% of the sigma computed using continuous 360 1 s samples at the three HI Island TGs with continuous 1 s samples (not shown). Local calibration is also needed to determine specific attenuation or amplification imparted by the TG protective well, which dampens oscillations <5 s and can create a resonance at periods near 5 s [*Park et al.*, 2014a]. For instance, regression (not shown) between hourly sigma computed by the NOAA TG acoustic sensor within its protective well and the subsurface Seabird pressure sensor are highly correlated, but reveal linear biases imparted by the protective well. Protective-well biases range from a 10% amplification with a 0.5 cm offset at the lower-energy harbor of Honolulu, Oahu to a 5% and 40% attenuation occurring at the higher-energy harbors of Hilo, Hawaii, and Kahului, Maui, respectively. NOAA is currently upgrading their TG network to a new sensor technology based upon microwave radars whose unobstructed measurement should eliminate most biases imparted by the protective well [*Park et al.*, 2014b].

Acknowledgments
We thank Mark Merrifield of the University of Hawaii Sea Level Center for sharing data and helpful comments and the Environmental Hydraulics Institute (IHCantabria) of the Universidad de Cantabria for providing its Global Ocean Wave (GOW) data.

References

Aucan, J. (2006), Directional wave climatology for the Hawaiian Islands from buoy data and the influence of ENSO on extreme wave events from model hindcast, *JCOMM Tech. Rep. 34/WMO-TD 1368*, World Meteorol. Organ., Geneva, Switzerland.

Aucan, J., R. Hoeke, and M. A. Merrifield (2012), Wave-driven sea level anomalies at the Midway tide gauge as an index of North Pacific storminess over the past 60 years, *Geophys. Res. Lett.*, *39*, L17603, doi:10.1029/2012GL052993.

Barnard, P. L., J. Allan, J. E. Hansen, G. M. Kaminsky, P. Ruggiero, and A. Doria (2011), The impact of the 2009–10 El Niño Modoki on U.S. West Coast beaches, *Geophys. Res. Lett.*, *38*, L13604, doi:10.1029/2011GL047707.

Bromirski, P. D., R. E. Flick, and D. R. Cayan (2003), Storminess variability along the California coast: 1858–2000, *J. Clim.*, *16*, 982–993.

Bromirski, P. D., D. R. Cayan, and R. E. Flick (2005), Wave spectral energy variability in the northeast Pacific, *J. Geophys. Res.*, *110*, C03005, doi:10.1029/2004JC002398.

Chawla, A., and L. H. Tolman (2008), Obstruction grids for spectral wave models, *Ocean Modell*, *22*(1–2), 12–25, doi:10.1016/j.ocemod.2008.01.003.

Church, J. A., et al. (2013), Sea level change, in *Climate Change 2013: The Physical Science Basis Contribution of Working Group I to the Fifth Assessment Report of the Intergovernmental Panel on Climate Change*, edited by T. F. Stocker et al., pp. 1137–1216, Cambridge Univ. Press, Cambridge, U. K.

CO-OPS (2001), Appendix A, in *Tidal Datums and Their Applications*, *Spec. Publ. NOS CO-OPS1*, pp. A1, NOAA, National Ocean Service Center for Operational Oceanographic Products and Services, Silver Spring, Md.

Ezer, T. (2015), Detecting changes in the transport of the Gulf Stream and the Atlantic overturning circulation from coastal sea level data: The extreme decline in 2009–2010 and estimated variations for 1935–2012, *Global Planet. Change*, *129*, 23–36.

Hoeke, R. K., K. L. McInnes, J. Kruger, R. McNaught, J. Hunter, and S. Smithers (2013), Widespread inundation of Pacific islands triggered by distant-source wind-waves, *Global Planet. Change*, *108*, 128–138, doi:10.1016/j.gloplacha.2013.06.006.

Marra, J. J., M. A. Merrifield, and W. V. Sweet (2012), Sea level and coastal inundation on pacific islands, in *Climate Change and Pacific Islands: Indicators and Impacts*, *Rep. 2012*, edited by V. W. Keener, Pacific Islands Regional Climate Assessment (PIRCA), Island Press, Washington, D. C.

Merrifield, M. A., P. R. Thompson, and M. Lander (2012), Multidecadal sea level anomalies and trends in the western tropical Pacific, *Geophys. Res. Lett.*, *39*, L13602, doi:10.1029/2012GL052032.

Merrifield, M. A., A. S. Genz, C. P. Kontoes, and J. J. Marra (2013), Annual maximum water levels from tide gauges: Contributing factors and geographic patterns, *J. Geophys. Res. Oceans*, *118*, 2535–2546, doi:10.1002/jgrc.20173.

Park, J., R. Heitsenrether, and W. Sweet (2014a), Microwave and acoustic water level and significant wave height estimates at NOAA tide stations, *J. Atmos. Oceanic Technol.*, *31*, 2294–2308.

Park, J., R. Heitsenrether, and W. Sweet (2014b), Water level and wave height estimates at NOAA tide stations from acoustic and microwave sensors, *NOAA Tech. Rep. NOS CO-OPS 075*, 41 p.

Park, J., W. V. Sweet, and R. Heitsenrether (2015), Water level oscillations in Monterey bay and harbor, *Ocean Sci.*, *11*, 439–453.

Parke, M. E., and S. K. Gill (1995), On the sea state dependence of sea level measurements at platform Harvest, *Mar. Geod.*, *18*, 105–111.

Perez, J., et al. (2015), Statistical multi-model climate projections of surface ocean waves in Europe, *Ocean Modell.*, doi:10.1016/j.ocemod.2015.06.001.

Ruggiero, P. (2013), Is the intensifying wave climate of the U.S. Pacific northwest increasing flooding and erosion risk faster than sea-level rise?, *J. Waterw Port Coastal Ocean Eng.*, *139*, 88–97, doi:10.1061/(ASCE)WW.1943-5460.0000172.

Salas, J. D., and J. Obeysekera (2013), Revisiting the concepts of return period and risk for nonstationary hydrologic extreme events, *J. Hydrol. Eng.*, doi:10.1061/(ASCE)HE.1943-5584.0000820.

Sweet, W. V., and J. Park (2014), From the extreme to the mean: acceleration and tipping points of coastal inundation from sea level rise, *Earth's Future*, *2*, 579–600.

Sweet, W. V., J. Park, J. J. Marra, C. Zervas, and S. Gill (2014), Sea level rise and nuisance flood frequency changes around the United States, *NOAA Tech. Rep. NOS CO-OPS 73*, 53 p.

Tebaldi, C., B. H. Strauss, and C. E. Zervas (2012), Modeling sea level rise impacts on storm surges along US coasts, *Environ. Res. Lett.*, *7*, 014032, doi:10.1088/1748-9326/7/1/014032.

Thotagamuwage, D. T., and C. B. Pattiaratchi (2014), Observations of infragravity period oscillations in a small marina, *Ocean Eng.*, *88*, 435–445.

Tolman, H. L. (2014), User manual and system documentation of WAVEWATCH III version 452 4.18, *NOAA/NWS /NCEP/MMAB Tech. Note 316*, pp. 194 + Appendices (pdf).

Vetter, O., J. M. Becker, M. A. Merrifield, A. C. Pequignet, J. Aucan, S. J. Boc, and C. E. Pollock (2010), Wave setup over a Pacific Island fringing reef, *J. Geophys. Res.*, *115*, C12066, doi:10.1029/2010JC006455.

Welch, P. D. (1967), The use of fast Fourier transform for the estimation of power spectra: A method based on time averaging over short, Modified Periodograms, *IEEE Trans. Audio Electroacoust.*, *AU-15*, 70–73.

Wijeratne, E. M. S., P. L. Woodworth, and D. T. Pugh (2010), Meteorological and internal wave forcing of seiches along the Sri Lanka coast, *J. Geophys. Res.*, *115*, C03014, doi:10.1029/2009JC005673.

Woodworth, P. L., D. T. Pugh, M. P. Meredith, and D. L. Blackman (2005), Sea level changes at Port Stanley, Falkland Islands, *J. Geophys. Res.*, *110*, C06013, doi:10.1029/2004JC002648.

Zervas, C. (2013), Extreme water levels of the United States 1893–2010, in *NOAA Tech. Rep. NOS CO-OPS 67*, 56 p., Appendices I-VIII.

Zhang, K., B. C. Douglas, and S. P. Leatherman (2000), Twentieth century storm activity along the U.S. East coast, *J. Clim.*, *13*, 1748–1760, doi:10.1175/1520-0442(2000)013<1748:TCSAAT>2.0.CO;2.